Selective Oxidation of Simple Aromatics Catalyzed by Nano-Biomimetic Metal Oxide Catalysts: A Mini Review

Wondemagegn H. Wanna [1†], Damodar Janmanchi [1†], Natarajan Thiyagarajan [1†], Ravirala Ramu [1,2], Yi-Fang Tsai [1] and Steve S. F. Yu [1*]

[1] Institute of Chemistry, Academia Sinica, Taipei, Taiwan, [2] Sree Dattha Institute of Engineering and Science, Hyderabad, India

The process of selective oxy-functionalization of hydrocarbons using peroxide, O_3, H_2O_2, O_2, and transition metals can be carried out by the reactive oxygen species such as hydroxyl/hydroperoxyl radical and/or metal oxygenated species generated in the catalytic reaction. Thus, a variety of mechanisms have been proposed for the selective catalytic oxidation of various hydrocarbons including light alkanes, olefins, and simple aromatics by the biological metalloproteins and their biomimetics either in their homogeneous or heterogeneous platforms. Most studies involving these metalloproteins are Fe or Cu monooxygenases. The pathways carried out by these metalloenzymes in the oxidation of C–H bonds invoke either radical reaction mechanisms including Fenton's chemistry and hydrogen atom transfer followed by radical rebound reaction mechanism or electrophilic oxygenation/O-atom transfer by metal-oxygen species. In this review, we discuss the metal oxide nano-catalysts obtained from metal salts/molecular precursors (M = Cu, Fe, and V) that can easily form *in situ* through the oxidation of substrates using $H_2O_{2(aq)}$ in CH_3CN, and be facilely separated from the reaction mixtures as well as recycled for several times with comparable catalytic efficiency for the highly selective conversion from hydrocarbons including aromatics to oxygenates. The mechanistic insights revealed from the oxy-functionalization of simple aromatics mediated by the novel biomimetic metal oxide materials can pave the way toward developing facile, cost-effective, and highly efficient nano-catalysts for the selective partial oxidation of simple aromatics.

Keywords: benzene, phenol, *p*-benzoquinone, hydrogen peroxide, toluene, metal oxide, nanocatalysts

INTRODUCTION

The technology of "advanced oxidation processes" essentially applies Fenton's chemistry for wastewater treatment (Andreozzi et al., 1999; Pignatello et al., 2006). The primary oxidants including O_3, H_2O_2, O_2, transition metal oxo-species, light, and electrical energy are employed to remove the organic (and sometimes inorganic) wastes in wastewater *via* the reactive oxygen species (ROS) and/or UV light (Deng and Zhao, 2015). These remediation processes can also be properly controlled and applied for the selective catalytic oxidation of hydrocarbons by designing variable homo- and heterogeneous catalyst systems to achieve green and environmentally benign fine chemical production (Ottenbacher et al., 2020; Suib et al., 2020).

In addition to accumulate ROS, it has been believed that the transition metals such as M = Fe, Cu, Co, and Mn in $H_2O_{2(aq)}$ can induce the metal oxygenates for the hydrocarbon activation (Sawyer et al., 1996). In fact, Fenton's chemistry can both possibly occur with the Haber–Weiss reaction mechanism (Equation 1) (Walling, 1975; Pignatello et al., 2006) for the accumulation of HO·/HOO· and for the formation ferryl-oxo species via Bray–Gorin mechanisms (Equation 2) (Bossmann et al., 1998; Enami et al., 2014). Interestingly, recent reports indicated the observation of Fenton's chemistry at the aqueous interface by mass spectrometry where there was no HO· observed but several ferryl-oxo species including dimeric forms were detected (Enami et al., 2014). The dimeric ferryl-oxo species are actually more reactive than the monomeric ferryl-oxo species for O-atom transfer (OAT) reaction. These further progresses in Fenton's chemistry have provided a significant insight to indicate the importance of the electronic coupling interplaying among the iron oxide clustering sites (Enami et al., 2014).

$$\mathbf{Fe^{II} + H_2O_2 \longrightarrow Fe^{III} + OH^- + \cdot OH} \qquad \textbf{(1)} \qquad \textbf{The Haber-Weiss mechanism}$$

$$\mathbf{Fe^{III} + H_2O_2 \longrightarrow Fe^{IV}O + H_2O} \qquad \textbf{(2)} \qquad \textbf{The Bray-Gorin mechanism}$$

For the selective oxidation of sp^2- vs. sp^3-carbons, "toluene" can be considered as a great example to illustrate the reaction behaviors mediated either by ROS or transition metal oxygenated species. If the reactions are mediated by ROS of HO· or HOO·, it may proceed either by the hydrogen atom transfer (HAT) of C–H bond in the methyl group and then radical rebound to form benzyl alcohol/benzyl hydroperoxide or direct addition of HO· to the sp^2 carbon center of o- or p-positions of the methyl substituent (**Figure 1**).

On the other hand, it has been long considered that the aromatic ring (sp^2 carbon) oxygenation mediated by the metalloproteins such as cytochrome P450 and toluene monooxygenase (ToMO) are proceeded with the formation of arene oxide and/or σ-complex intermediates via OAT then 1,2-hydride shift (NIH shift rearrangement) toward the formation of phenolate products (Guroff et al., 1967; Boyd et al., 1972; Jerina and Daly, 1974; Bassan et al., 2003; de Visser and Shaik, 2003; Mitchell et al., 2003). With respect to sp^3 C–H bond activation, the oxidation may directly be conducted by the high valent iron oxo or ferryl-oxo species either through HAT or OAT reaction mechanism (Bassan et al., 2003; de Visser and Shaik, 2003). In any case, the formation of benzaldehyde can be subsequently produced by oxidation through HAT and radical rebound or OAT toward the methylene C–H bond of benzyl alcohol (**Figure 1**). The bond dissociation energy (BDE = 86–89 kcal/mol) of C–H bond in methyl substituent of toluene is much lower than the ring activation of toluene (BDE = 109–112 kcal/mol) (Bassan et al., 2003; de Visser and Shaik, 2003).

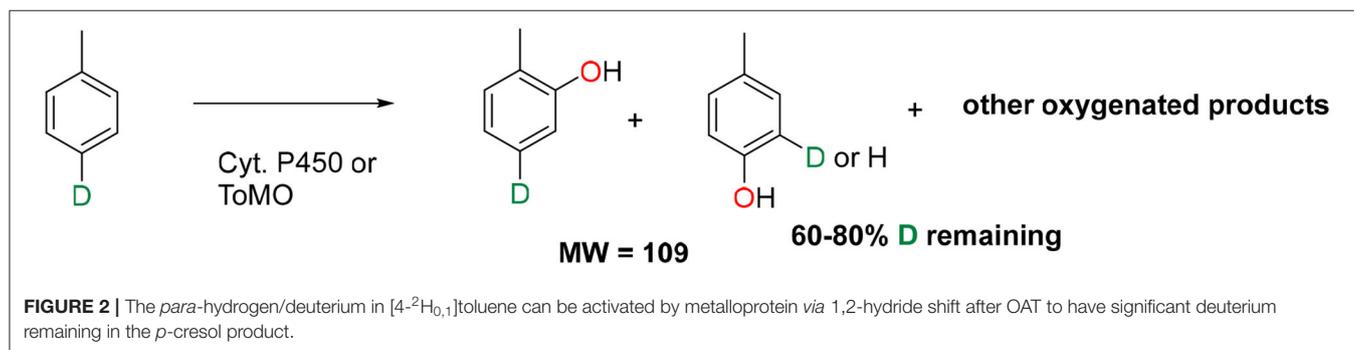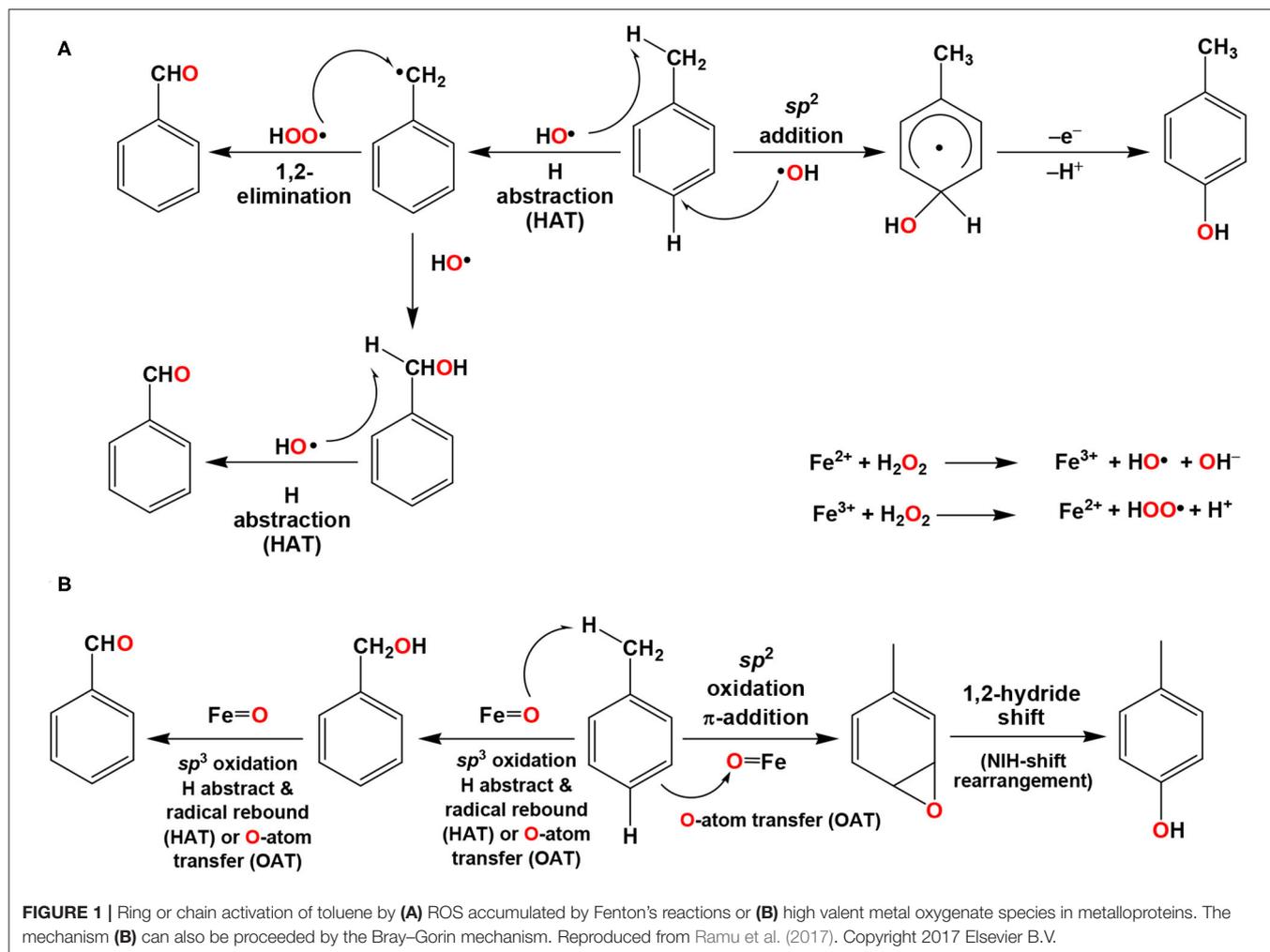The significant mechanistic feature for OAT ring oxidation can be easily determined by enriched aromatics with a deuterium atom at the site/position for oxidation (Ramu et al., 2017). For toluene oxidation using $H_2O_{2(aq)}$, the sp^2 activated site usually appeared either at the o- or p-position; therefore, $[4-^2H_{0,1}]$ toluene can be synthesized from 4-bromo-toluene in D_2O (Morimoto et al., 2015) and used as a mechanistic probe to evidence the OAT mechanism if there is significant proportion of deuterium that remained in the molecules (**Figure 2**). Usually, the NIH shift ratios for metalloproteins can be up to 60–80% (Guroff et al., 1967; Boyd et al., 1972; Siegmund and Kaufman, 1991; Mitchell et al., 2003).

It is worth noting that in the past study, the addition of CH_3CN to Fenton's reaction mixtures can enhance the NIH shift ratios from <5%, for Fe^{II} in aqueous solution, i.e., Fenton's oxidation, up to 50% (Castle et al., 1980; Kurata et al., 1988). These phenomena have made us wonder whether the corresponding reaction conditions can significantly accumulate any metal oxygenated species like metalloproteins of cytochrome P450 or ToMO. If so, then, how can we control the accumulated reactive oxygenated species for selective sp^3 C–H vs. sp^2 C–H bond oxidation via HAT or π-bond activation via OAT?

SELECTIVE OXIDATION OF sp^2 AND sp^3 C–H BOND OXIDATION OF TOLUENE BY NANO-IRON OXIDE PARTICLES

Molecular iron complexes including polycyclic cage-like compounds, biomimetic model complexes, and encapsulated within zeolite cages have been shown with high catalytic activity in the oxidation of hydrocarbons including alkanes and aromatics (Mori et al., 2008; Bilyachenko et al., 2016; Yalymov et al., 2017; Zhang et al., 2017). Recently, we indicated that $Fe(ClO_4)_2$ salt using $H_2O_{2(aq)}$ in CH_3CN can conduct selective oxidation of toluene either for sp^2 C–H bond oxidation to cresols or sp^3 C–H bond oxidation to benzyl alcohol/benzaldehyde (Ramu et al., 2017). Interestingly, the slow addition of $H_2O_{2(aq)}$ to the reaction mixtures led to π-activation (∼70%) for cresols/methyl-p-benzoquinone (BQ) formation, whereas the fast addition of $H_2O_{2(aq)}$ resulted in the major production sp^3 C–H bond oxidation at the methyl substituent (Ramu et al., 2017). Further scrutinizing the reaction mixture by the electron microscopic (EM) study revealed small nanoparticle formation with the sizes of 2–10 nm in the first 2 h with the slow addition of $H_2O_{2(aq)}$ (**Supplementary Figure 1A**, **Supplementary Information**) and relatively larger particles of >1 μm were observed within 2 h after the fast addition of $H_2O_{2(aq)}$ (**Supplementary Figure 1B**, **Supplementary Information**). These particles were

FIGURE 1 | Ring or chain activation of toluene by **(A)** ROS accumulated by Fenton's reactions or **(B)** high valent metal oxygenate species in metalloproteins. The mechanism **(B)** can also be proceeded by the Bray–Gorin mechanism. Reproduced from Ramu et al. (2017). Copyright 2017 Elsevier B.V.

FIGURE 2 | The *para*-hydrogen/deuterium in [4-^{2}H$_{0,1}$]toluene can be activated by metalloprotein *via* 1,2-hydride shift after OAT to have significant deuterium remaining in the *p*-cresol product.

evidenced to be consisted of iron oxides from transmission electron microscopy (TEM), energy-dispersive X-ray (**Supplementary Figure 2**, **Supplementary Information**), and elemental analysis (**Supplementary Table 1**, **Supplementary Information**) study. It is not surprising that with the fast addition of $H_2O_{2(aq)}$, exothermic heat accumulated for the micro-size iron oxide nanoparticle formation, substantial amounts of HO·/HOO· were generated and the overall sp^3

oxidation products can achieve >95%. To further examine the production of benzyl hydroperoxide, the treatment of PPh$_3$ can further assist for its quantification (Shul'pin et al., 2010). Once the reaction is harvested, a very small amount of benzyl hydroperoxide species was observed in rapid addition of $H_2O_{2(aq)}$. However, with slow addition of $H_2O_{2(aq)}$, ~45% sp^3 C–H bond oxidation products were observed, and the ratios for benzyl hydroperoxide, benzaldehyde, and benzyl

alcohol were identified to be 18, 25, and 2%, respectively (**Supplementary Table 2**, **Supplementary Information**). Nevertheless, the selectivity for sp^2 carbon oxidation to cresols/methyl-p-BQ formation, with and without treatment of PPh$_3$ after the reactions, did not vary much with rapid or slow additions of H$_2$O$_{2(aq)}$.

The study using [4-^{2}H$_{0,1}$]toluene for its oxidation catalyzed by Fe(ClO$_4$)$_2$ catalyst using H$_2$O$_2$ in CH$_3$CN exhibited high NIH-shift ratios of 83–86% (Ramu et al., 2017). On further examination using the resulted iron nanoparticles, the selectivity for sp^2 C–H bond oxidation in cresols/p-BQ formations can still reach 65% (**Supplementary Table 3**, **Supplementary Information**) where the obtained NIH-shift ratio of deuterium remaining for p-cresol product is 81% (**Supplementary Information**). The outcome here implicated that the activation of aromatic π-bonds for arene oxide or σ-complex may be mediated by iron-based oxygenated species (Kudrik and Sorokin, 2008; Thibon et al., 2012; Raba et al., 2014) that was presumably arisen from the resultant particle surface of the iron nanoparticle.

HIGHLY SELECTIVE OXIDATION OF BENZENE TO p-BENZOQUINONE (p-BQ) BY COPPER OXIDE NANO-CATALYST

Multi-copper complexes including cage compounds were employed for selective oxidation of alkanes and aromatics with H$_2$O$_{2(aq)}$ in CH$_3$CN (You et al., 2014; Kulakova et al., 2017, 2019). Shul'pin and co-workers further reported a double oxidation from benzene to p-BQ with molar ratio of ∼1:1 (PhOH:p-BQ) using Cu(ClO$_4$)$_2$ (Shul'pina et al., 2008). Similarly, a series of tri-copper cluster complexes achieved an efficient conversion of benzene to p-hydroquinone with percentage selectivity of 60–98% (Nagababu et al., 2012). Recently, we have discovered and studied copper oxide–based nano-catalysts for the efficient and selective double oxidation from benzene to p-BQ. During the process, the addition of optimized amount of H$_2$O in the CH$_3$CN solution with copper nanoparticles yielded higher overall catalytic efficiency yield based on consumed H$_2$O$_2$ value (98%), and better selectivity for p-BQ (77%), than other volumes of water (Wanna et al., 2019b). Most importantly, we were able to recycle the catalyst at least three times without significantly losing activity and p-BQ selectivity.
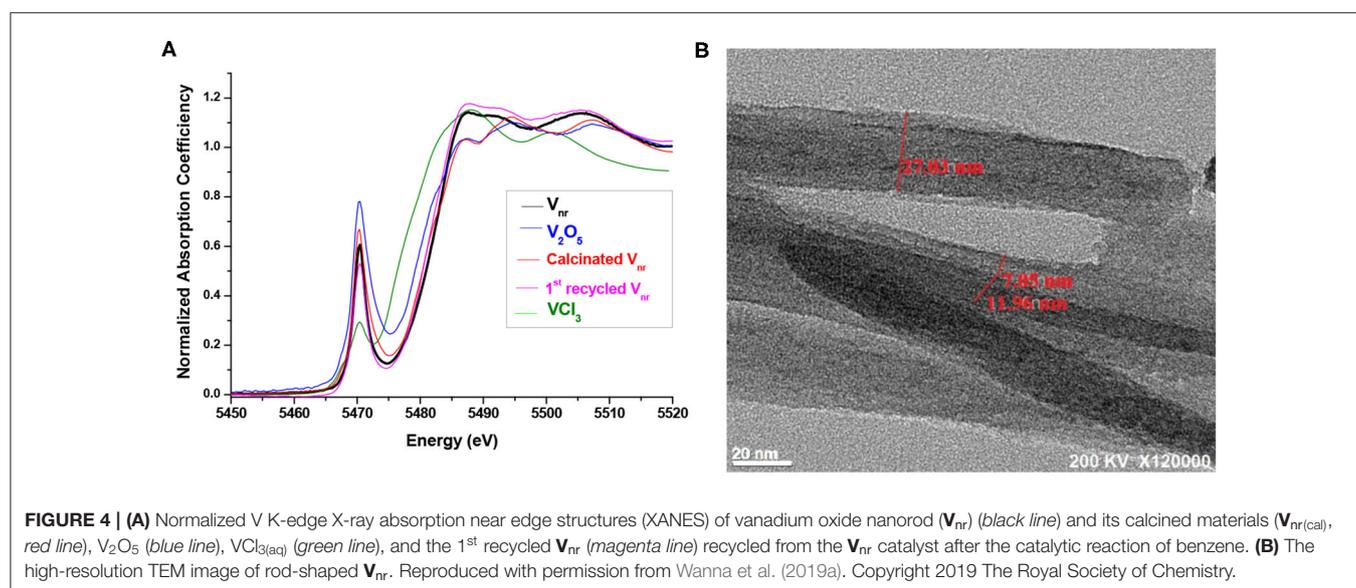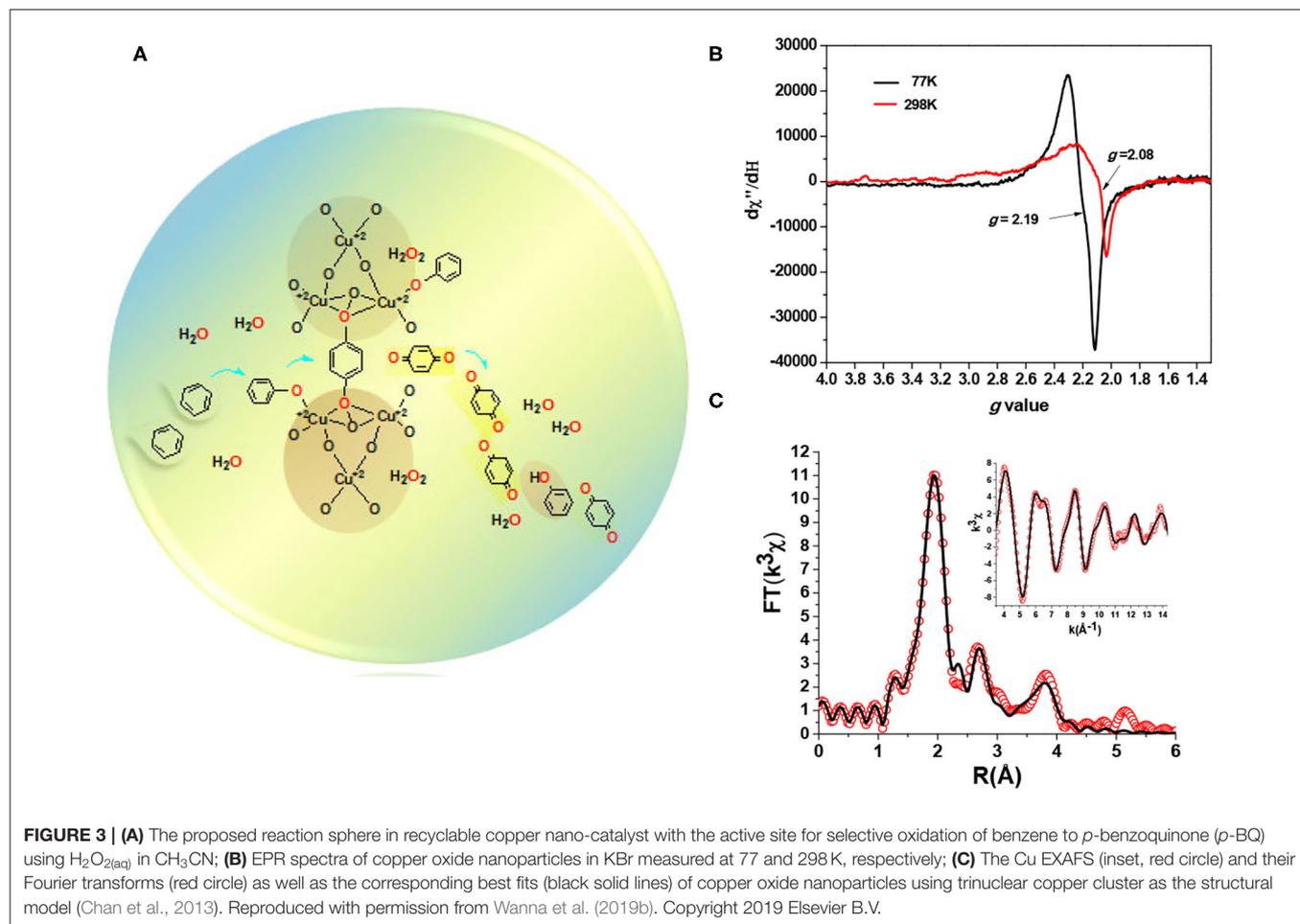
The EPR spectrum of copper oxide nanoparticles at 298 K indicated an isotropic signal, reminiscent of a previous study of pMMO with trinuclear copper cluster feature (Nguyen et al., 1994), which was significantly broadened and presented relatively poor signal-to-noise ratio than the one at 77 K (**Figure 3B**) (Wanna et al., 2019b). The result here reveals substantial dynamic motions around the metal centers, which are behaving like metal active sites in the metallo-monooxygenases (Chen et al., 2014; Wang et al., 2017; Yang et al., 2017). In addition, the corresponding EXAFS data fittings (k^3-weighted) using two structural models of copper oxide and trinuclear copper cluster model (Cu$_{2.8}$O$_{4.6}$), respectively, can both give reasonable fits of R_{fit} = 0.027 and 0.15%, respectively (Wanna et al.,

2019b), which indicated that a trinuclear copper cluster feature is manifested from the obtained oxide materials (**Figure 3**). Especially, the specific Cu–Cu scattering in a distance of ∼3.7 Å would presumably result in Cu^{2+}(μ-(η^2:η^2)-peroxo)Cu^{2+} (Cu–Cu distance ∼3.6 Å) that can potentially reach an equilibrium of a Cu^{3+}(μ-O)$_2$Cu^{3+} structure (Lewis and Tolman, 2004; Mirica et al., 2004; Ottenwaelder et al., 2006). The formed possible intermediate of Cu^{2+}Cu^{2+}(μ-O)$_2$Cu^{3+} can exhibit much lower activation energy for a facile oxo-transfer toward the inert C–H bond (Chen and Chan, 2006). It is not surprising that a benzene molecule can therefore easily possess an arene oxide intermediate *via* OAT followed by subsequent NIH rearrangement to obtain PhOH from benzene. In fact, the recycled copper nanoparticles performed with reasonable efficiency in toluene oxidation. The NIH-shift ratios obtained from the deuterated p-cresol products was 54%, which displayed that the solid-state surface of copper nanoparticles can in general oxidize *ortho*- or *para*- (sp^2) C–H bonds of toluene *via* the formation of arene oxide intermediate followed by an NIH rearrangement process.

THE MIXED VALENCE SITES OF V^{4+}/V^{5+} STABILIZED BY PCA IN THE V$_2$O$_5$ FOR SELECTIVE OXIDATION OF BENZENE TO PHENOL WITH HIGH EFFICIENCY

Vanadium-based polyoxometalates have been extensively used as green heterogeneous catalysts with high catalytic activity for selective oxidation of styrene to benzaldehyde (Zhou et al., 2020), benzene to PhOH (Li et al., 2020), and mono-substituted benzene to p-PhOH (Kamata et al., 2012). Kirillov and Shul'pin (2013) established a variety of vanadium complexes to catalyze aerobic and/or H$_2$O$_2$ hydroxylation of benzene to phenol and toluene to a mixture of cresols in CH$_3$CN. Mandatory promoters such as pyridine, pyrazine-2-carboxylic acid (PCA), and acetic acid were used as co-catalysts to prompt the oxidation reactions. We recently reported a unique vanadium nanorod (V_{nr}) catalyst (**Figure 4B**) for selective oxidation of benzene to PhOH (>87%) with minor p-BQ formation in CH$_3$CN. The presence of PCA, interacting V^{+4}/V^{+5} in V_{nr}, can serve as Brønsted acid site to improve activity for PhOH production (Liu et al., 2017; Zhao et al., 2018). In fact, PCA ligand can serve as a stabilizer of the transition state involving V^{4+} species for the H-transfer (Kirillova et al., 2009) and the reduction of V^{5+} to V^{4+} by PCA with H$_2$O$_{2(aq)}$ assists in accumulating more redox active centers (Shul'pin et al., 1999). During the detailed characterization of V$_2$O$_5$-related materials, including the V_{nr} catalyst prepared from VCl$_3$, we found that lower pre-edge peak intensity of XAS data at ∼5,470 eV together with XPS data analysis indicated V_{nr} catalyst exhibited higher V^{+4}/V^{+5} ratio than the "calcined V_{nr}" ($V_{nr(cal)}$) and commercial V$_2$O$_5$ (**Figure 4A**). For the efficient conversion of benzene to PhOH, assisted by PCA, the vanadium materials exhibit high dependence on V^{+4}/V^{+5} ratios (**Table 1**).

V_{nr} catalyst can also conduct toluene oxidation and its selective sp^2 C–H bond oxidation or π-activation for cresols/methyl-p-BQ formation up to 52% assisted by PCA (Wanna et al., 2019a). For 48% sp^3 C–H bond oxidation

FIGURE 3 | (A) The proposed reaction sphere in recyclable copper nano-catalyst with the active site for selective oxidation of benzene to *p*-benzoquinone (*p*-BQ) using $H_2O_{2(aq)}$ in CH_3CN; **(B)** EPR spectra of copper oxide nanoparticles in KBr measured at 77 and 298 K, respectively; **(C)** The Cu EXAFS (inset, red circle) and their Fourier transforms (red circle) as well as the corresponding best fits (black solid lines) of copper oxide nanoparticles using trinuclear copper cluster as the structural model (Chan et al., 2013). Reproduced with permission from Wanna et al. (2019b). Copyright 2019 Elsevier B.V.

FIGURE 4 | (A) Normalized V K-edge X-ray absorption near edge structures (XANES) of vanadium oxide nanorod (**V**$_{nr}$) (*black line*) and its calcined materials (**V**$_{nr(cal)}$, *red line*), V_2O_5 (*blue line*), $VCl_{3(aq)}$ (*green line*), and the 1st recycled **V**$_{nr}$ (*magenta line*) recycled from the **V**$_{nr}$ catalyst after the catalytic reaction of benzene. **(B)** The high-resolution TEM image of rod-shaped **V**$_{nr}$. Reproduced with permission from Wanna et al. (2019a). Copyright 2019 The Royal Society of Chemistry.

products, in comparison with the product ratio by the addition of PPh$_3$ after the reaction, the ratios for benzaldehyde and benzyl hydroperoxide were identified to be 23 and 25%, respectively (**Supplementary Table 2**, **Supplementary Information**). In addition, high NIH rearrangement ratio of 80% suggests that the reaction mechanism for *sp*^{2} C–H bond oxidation/π activation

TABLE 1 | The summary of X-ray photoelectron spectroscopy (XPS) and X-ray absorption spectroscopy (XAS) data of vanadium oxide catalysts including V_{nr} and its reactivity parameters.

Catalysts	XPS	Normalized XAS intensity	Gain factor[a]	Selectivity[b] (%)	TONs[c] of PhOH
	V^{4+}/V^{5+} ratio	5,470 eV			
V_{nr}	0.301	0.61	0.13	87	11.7
V_{nr}(PCA)	0.301	0.61	0.64	95	25.5
1st recycled V_{nr} (PCA)	0.639	0.53	0.31	91	20.3
$V_{nr(cal)}$ (PCA)	0.218	0.67	0.23	94	17.1
V_2O_5 commercial (PCA)	0.118	0.78	0.09	95	9.6

[a]Gain factor = (mol of oxygenated product)/(mol of H_2O_2 consumed). [b]Selectivity of PhOH = [(PhOH) (mol)/[p-BQ + PhOH] (mol)] × 100. [c]Turnover number (TON) for PhOH was determined by calculating the number of millimoles of product per millimole of catalyst (based on V content).

of toluene, presumably, also contributed partly to the catalytic oxidation of benzene to phenol, mainly *via* an electrophilic OAT of vanadium hydroperoxide or high valent vanadium oxo intermediates. The oxidation of benzene to PhOH catalyzed by V_{nr} catalyst using $H_2^{18}O_{2(aq)}$ as an oxidant displayed 68% ^{18}O-enriched PhOH; however, there was negligible enrichment using $H_2^{16}O_2$ and $^{18}O_2$. The results implicate $H_2O_{2(aq)}$ as the essential oxidant for OAT mediated by the vanadium oxygenated species.

CHARACTERIZATIONS AND COMMON FEATURES OF THE Fe/Cu/V NANO-CATALYSTS

The Fe, Cu, and V oxide nano-catalysts as a type of metal oxide material possessed metal-oxygen/hydroxide components that can be polymerized and form active hybrid materials with oxygenated hydrocarbons (**Supplementary Figures 1–7, Supplementary Information**). N_2 adsorption–desorption isotherms and XRD studies reveal the porous structure and crystalline feature of these catalysts that formed from the core metal oxide with the organic linker as a framework. These three catalysts similarly possessed mesoporous structure in a pore size range of 1.5–30 nm and BET surface area of each was in the range of 20–30 m^2/g that can be essential for catalytic activation of the small aromatic compounds. The mesopore structure of the catalysts has a type of slit-like pore formed by the effect of substrate (benzene/toluene) acting as template while preparing *in situ* (Rouquerol et al., 1994; Thommes et al., 2015; Wanna et al., 2019a,b). The porous property observed in these Fe/Cu/V nano-catalysts contributed to the improvement of benzene oxidation efficiency using $H_2O_{2(aq)}$ with additional H_2O proportions in CH_3CN (Ramu et al., 2017; Wanna et al., 2019b), which is consistent with the effect of water-assisted benzene oxidation catalyzed by the molecular iron complex encapsulated in the zeolite (Yamaguchi et al., 2015). In addition, the powder XRD and selected area (electron) diffraction SAD-TEM analysis for V_{nr} catalyst indicated that the crystal grew longer to rod shape with preferential (220) orientation that can be crucial for the related additional activities (Berenguer et al., 2017). The crystalline feature of Fe and Cu catalysts also exhibited a

distinctive crystal arrangement that directly corresponded to the nature of the parental metal-oxide materials.

Thermogravimetric analysis study of the organic composition of the nano-catalysts indicates that it accounts for 10–50% and plays key roles for structural framework formation and selective catalytic activity (**Supplementary Figures 3, 5, 7, Supplementary Information**) (Zoubi et al., 2009; Wanna et al., 2019a,b). Calcination of these catalysts at 500°C under N_2 completely decomposes the organic linker, collapses the structural framework, and changes the surface morphology that causes a decline in catalytic activity significantly. In the XPS investigation of the catalysts' surface, beside the common metal-oxide/hydroxide functional groups, we identified a hydrocarbon group that offers hydrophobic surfaces (Wanna et al., 2019a,b) that are crucial for high dispersion of the nanoparticles and surface–substrate interaction (Wu et al., 2006; Biesinger et al., 2007; Dong et al., 2016). The central metal-oxide cluster in support with the organic linker forms the surface atomic structure that can be active for catalytic application. In addition to this, XPS and XAS studies show coexistence of the mixed valance states such as Fe^{2+}/Fe^{3+}, Cu^+/Cu^{2+}, and V^{4+}/V^{5+} that are essential for C–H or π-bond activation.

DISCUSSION

Overall, the study provides an efficient strategy that accumulates active Fe, Cu, and V oxide species of organic–inorganic hybrid nano-catalysts, respectively, through the addition of 35% $H_2O_{2(aq)}$ to the Fe/Cu perchlorate and VCl_3 in CH_3CN for the selective oxidation of simple aromatics (Ramu et al., 2017; Wanna et al., 2019a,b). Interestingly, these metal nanoparticles can be further recycled several times that can carry out the selective catalytic oxidation of benzene to PhOH or p-BQ and toluene to cresols/methyl-p-BQ (sp^2 C–H bond oxidation) or benzyl alcohol/benzaldehyde (sp^3 C–H bond oxidation). This indicates that, in the presence of organic residues including CH_3CN, benzene, and/or toluene, the oxidant of $H_2O_{2(aq)}$ can not only accumulate HO·/HOO· but is also essential for the self-assembly of the heterogeneous metal-oxide hybrid catalyst formation with active metal oxygenated species.

CH_3CN is a polar solvent that can be miscible with polar H_2O_2 and H_2O as well as the non-polar aromatic substrates,

leading to oxygenate formation. When the metal salts dissolved in the reaction mixtures of aromatics, the free Cu/Fe/V ions presumably coordinate with CH_3CN serving as a ligand to form metal complexes (Rach and Kühn, 2009; Kulakova et al., 2017). As V_{nr} catalyst can be directly prepared from $H_2O_{2(aq)}$ in CH_3CN without any additional substrates (Wanna et al., 2019a), we therefore surmise that these CH_3CN-based metal complexes in the presence of $H_2O_{2(aq)}$ can occur and are essential to assist the metal oxide polymerization/formation.

In addition, it has already been known that catalytic aromatic hydroxylation with $H_2O_{2(aq)}$ is the cause of further oxidation of initially formed phenols and the appearance of tar (Olah et al., 1981; Kholdeeva, 2015). As long as we take into consideration this additional factor in a heterogeneous platform for the metal catalyzed oxidation or the reaction condition for Fenton's chemistry, the accumulated ROS exerted on the oxide surface may not be considered as diffusible radicals anymore. The Cu and Fe nanoparticles can achieve the oxidation of toluene for o,p-cresols in 75% selectivity whereas for the V_{nr} materials, it is ~52%. The NIH-shift ratios obtained from the mechanistic probe of $[4\text{-}^2H_{0,1}]$toluene catalyzed by Fe, Cu, and V nano-catalysts are ~85, 57, and 80%, respectively (Ramu et al., 2017; Wanna et al., 2019a,b). The results further support that the oxidation using $H_2O_{2(aq)}$ in CH_3CN catalyzed by the metal oxide nano-catalysts can give rise to reactivity from the specific $Fe^{IV} = O$ species on poly-iron oxo clusters (Enami et al., 2014) as evidenced from EM studies, tri-copper cluster moiety that existed in the copper oxide assembled nanoparticles (Wanna et al., 2019b), and crucial V^{4+}/V^{5+} redox sites stabilized by PCA (Wanna et al., 2019a), which can significantly undergo OAT process for aromatics activation via the arene oxide intermediates (Guroff et al., 1967; Jerina and Daly, 1974; Bassan et al., 2003).

In summary, highly dispersed active Fe, Cu, and V nano-catalysts with H_2O_2/O_2, in a heterogeneous platform, can drive selective oxidation of simple aromatics such as benzene and toluene. Furthermore, these unique catalysts effectively tuned sp^2 vs. sp^3 C–H bond hydroxylation of toluene and achieved selective double oxidation of benzene to p-BQ. In many cases, the reaction mechanism proceeds significantly through OAT process

via the formation of the arene oxide intermediate, although the free radicals that initiated oxidation of C–H bond also participate. These nano-catalysts prepared $in situ$ and composed of organic–inorganic hybrid exhibited recyclable properties, controlled selectivity, higher activity, and were greener than their bulk oxide counterparts, which make them potentially promising for large-scale application.

AUTHOR CONTRIBUTIONS

WW, DJ, NT, and RR conducted the research of catalytic oxidative conversion of simple aromatics. WW, DJ, NT, RR, and Y-FT carried out the identification and characterization of the metal oxide materials. SY organized the research. WW, DJ, NT, and SY wrote the paper. All authors contributed to the article and approved the submitted version.

FUNDING

ACKNOWLEDGMENTS

SUPPLEMENTARY MATERIAL

The Supplementary Material for this article can be found online at: https://www.frontiersin.org/articles/10.3389/fchem.2020.589178/full#supplementary-material

REFERENCES

Andreozzi, R., Caprio, V., Insola, A., and Marotta, R. (1999). Advanced oxidation processes (AOP) for water purification and recovery. *Catal. Today* 53, 51–59. doi: 10.1016/S0920-5861(99)00102-9

Bassan, A., Blomberg, M. R. A., and Siegbahn, P. E. M. (2003). Mechanism of aromatic hydroxylation by an activated Fe^{IV} =O core in tetrahydrobiopterin-dependent hydroxylases. *Chem. Eur. J.* 9, 4055–4067. doi: 10.1002/chem.200304768

Berenguer, R., Guerrero-Pérez, M. O., Guzmán, I., Rodríguez-Mirasol, J., and Cordero, T. (2017). Synthesis of vanadium oxide nanofibers with variable crystallinity and V^{5+}/V^{4+} Ratios. *ACS Omega* 2, 7739–7745. doi: 10.1021/acsomega.7b01061

Biesinger, M. C., Hart, B. R., Polack, R., Kobe, B. A., and Smart, R. S. C. (2007). Analysis of mineral surface chemistry in flotation separation using imaging XPS. *Min. Eng.* 20, 152–162. doi: 10.1016/j.mineng.2006.08.006

Bilyachenko, A. N., Levitsky, M. M., Yalymov, A. I., Korlyukov, A. A., Khrustalev, V. N., Vologzhanina, A. V., et al. (2016). Cage-like Fe,Na-germsesquioxanes:

structure, magnetism, and catalytic activity. *Angew. Chem. Int. Ed.* 55, 15360–15363. doi: 10.1002/anie.201607189

Bossmann, S. H., Oliveros, E., Göb, S., Siegwart, S., Dahlen, E. P., Payawan, L., et al. (1998). New evidence against hydroxyl radicals as reactive intermediates in the thermal and photochemically enhanced fenton reactions. *J. Phys. Chem. A* 102, 5542–5550. doi: 10.1021/jp980129j

Boyd, D. R., Daly, J. W., and Jerina, D. M. (1972). Rearrangement of (1-^2H)- and (2-^2H)naphthalene 1,2-oxides to 1-naphthol. Mechanism of the NIH shift. *Biochemistry* 11, 1961–1966. doi: 10.1021/bi00760a035

Castle, L., Lindsay Smith, J. R., and Buxton, G. V. (1980). Aromatic hydroxylation by oxy-radicals — a possible model for hydroxylation catalysed by cytochrome P450. *J. Mol. Catal.* 7, 235–243. doi: 10.1016/0304-5102(80)85021-8

Chan, S. I., Lu, Y. J., Nagababu, P., Maji, S., Hung, M. C., Lee, M. M., et al. (2013). Efficient oxidation of methane to methanol by dioxygen mediated by tricopper clusters. *Angew. Chem. Int. Ed.* 52, 3731–3735. doi: 10.1002/anie.201209846

Chen, P. P. Y., and Chan, S. I. (2006). Theoretical modeling of the hydroxylation of methane as mediated by the particulate methane monooxygenase. *J. Inorg. Biochem.* 100, 801–809. doi: 10.1016/j.jinorgbio.2005.12.014

Chen, Y. S., Luo, W. I., Yang, C. L., Tu, Y. J., Chang, C. W., Chiang, C. H., et al. (2014). Controlled oxidation of aliphatic C-H bonds in metallo-monooxygenases: mechanistic insights derived from studies on deuterated and fluorinated hydrocarbons. *J. Inorg. Biochem.* 134, 118–133. doi: 10.1016/j.jinorgbio.2014.02.005

de Visser, S. P., and Shaik, S. (2003). A proton-shuttle mechanism mediated by the porphyrin in benzene hydroxylation by cytochrome P450 enzymes. *J. Am. Chem. Soc.* 125, 7413–7424. doi: 10.1021/ja034142f

Deng, Y., and Zhao, R. (2015). Advanced oxidation processes (AOPs) in wastewater treatment. *Curr. Pollut. Rep.* 1, 167–176. doi: 10.1007/s40726-015-0015-z

Dong, Y., Niu, X., Song, W., Wang, D., Chen, L., Yuan, F., et al. (2016). Facile synthesis of vanadium oxide/reduced graphene oxide composite catalysts for enhanced hydroxylation of benzene to phenol. *Catalysts* 6:74. doi: 10.3390/catal6050074

Enami, S., Sakamoto, Y., and Colussi, A. J. (2014). Fenton chemistry at aqueous interfaces. *Proc. Nat. Acad. Sci. U.S.A.* 111, 623–628. doi: 10.1073/pnas.1314885111

Guroff, G., Renson, J., Udenfriend, S., Daly, J. W., Jerina, D. M., and Witkop, B. (1967). Hydroxylation-induced migration: the NIH Shift. *Science* 157, 1524–1530. doi: 10.1126/science.157.3796.1524

Jerina, D. M., and Daly, J. W. (1974). Arene oxides: a new aspect of drug metabolism. *Science* 185, 573–582. doi: 10.1126/science.185.4151.573

Kamata, K., Yamaura, T., and Mizuno, N. (2012). Chemo- and regioselective direct hydroxylation of arenes with hydrogen peroxide catalyzed by a divanadium-substituted phosphotungstate. *Angew. Chem. Int. Ed.* 51, 7275–7278. doi: 10.1002/anie.201201605

Kholdeeva, O. A. (2015). "Selective Oxidation of Aromatics Rings," in *Arene Chemistry: Reaction Mechanisms and Methods for Aromatic Compounds, 1st Edn*, ed J. Mortier (Hoboken, NJ: John Wiley & Sons, Inc.), 365–398. doi: 10.1002/9781118754887.ch14

Kirillov, A. M., and Shul'pin, G. B. (2013). Pyrazinecarboxylic acid and analogs: highly efficient co-catalysts in the metal-complex-catalyzed oxidation of organic compounds. *Coord. Chem. Rev.* 257, 732–754. doi: 10.1016/j.ccr.2012.09.012

Kirillova, M. V., Kuznetsov, M. L., Romakh, V. B., Shul'pina, L. S., Fraústo Da Silva, J. J. R., Pombeiro, A. J. L., et al. (2009). Mechanism of oxidations with H_2O_2 catalyzed by vanadate anion or oxovanadium(V) triethanolaminate (vanadatrane) in combination with pyrazine-2-carboxylic acid (PCA): kinetic and DFT studies. *J. Catal.* 267, 140–157. doi: 10.1016/j.jcat.2009.08.006

Kudrik, E. V., and Sorokin, A. B. (2008). N-Bridged diiron phthalocyanine catalyzes oxidation of benzene with H_2O_2 via benzene oxide with NIH shift evidenced by using 1,3,5-[D_3]benzene as a probe. *Chem. Eur. J.* 14, 7123–7126. doi: 10.1002/chem.200800504

Kulakova, A. N., Bilyachenko, A. N., Levitsky, M. M., Khrustalev, V. N., Korlyukov, A. A., Zubavichus, Y. V., et al. (2017). $Si_{10}Cu_6N_4$ cage hexacoppersilsesquioxanes containing N ligands: synthesis, structure, and high catalytic activity in peroxide oxidations. *Inorg. Chem.* 56, 15026–15040. doi: 10.1021/acs.inorgchem.7b02320

Kulakova, A. N., Korlyukov, A. A., Zubavichus, Y. V., Khrustalev, V. N., Bantreil, X., Shul'pina, L. S., et al. (2019). Hexacoppergermsesquioxanes as complexes with N-ligands: synthesis, structure and catalytic properties. *J. Organometal. Chem.* 884, 17–28. doi: 10.1016/j.jorganchem.2019.01.004

Kurata, T., Watanabe, Y., Katoh, M., and Sawaki, Y. (1988). Mechanism of aromatic hydroxylation in the Fenton and related reactions. One-electron oxidation and the NIH shift. *J. Am. Chem. Soc.* 110, 7472–7478. doi: 10.1021/ja00230a032

Lewis, E. A., and Tolman, W. B. (2004). Reactivity of dioxygen–copper systems. *Chem. Rev.* 104, 1047–1076. doi: 10.1021/cr020633r

Li, X., Xue, H., Lin, Q., and Yu, A. (2020). Amphiphilic poly(ionic liquid)/wells–dawson-type phosphovanadomolybdate ionic composites as efficient and recyclable catalysts for the direct hydroxylation of benzene with H_2O_2. *Appl. Organometal. Chem.* 34:e5606. doi: 10.1002/aoc.5606

Liu, M. S., Su, B., Tang, Y., Jiang, X. C., and Yu, A. B. (2017). Recent advances in nanostructured vanadium oxides and composites for energy conversion. *Adv. Energy Mater.* 7:1700885. doi: 10.1002/aenm.201700885

Mirica, L. M., Ottenwaelder, X., and Stack, T. D. P. (2004). Structure and spectroscopy of copper–dioxygen complexes. *Chem. Rev.* 104, 1013–1046. doi: 10.1021/cr020632z

Mitchell, K. H., Rogge, C. E., Gierahn, T., and Fox, B. G. (2003). Insight into the mechanism of aromatic hydroxylation by toluene 4-monooxygenase by use of specifically deuterated toluene and p-xylene. *Proc. Natl. Acad. Sci. U.S.A.* 100, 3784–3789. doi: 10.1073/pnas.0636619100

Mori, K., Kagohara, K., and Yamashita, H. (2008). Synthesis of tris(2,2'-bipyridine)iron(II) complexes in zeolite Y cages: influence of exchanged alkali metal cations on physicochemical properties and catalytic activity. *J. Phys. Chem. C* 112, 2593–2600. doi: 10.1021/jp709571v

Morimoto, Y., Bunno, S., Fujieda, N., Sugimoto, H., and Itoh, S. (2015). Direct hydroxylation of benzene to phenol using hydrogen peroxide catalyzed by nickel complexes supported by pyridylalkylamine ligands. *J. Am. Chem. Soc.* 137, 5867–5870. doi: 10.1021/jacs.5b01814

Nagababu, P., Maji, S., Kumar, M. P., Chen, P. P. Y., Yu, S. S. F., and Chan, S. I. (2012). Efficient room-temperature oxidation of hydrocarbons mediated by tricopper cluster complexes with different ligands. *Adv. Synth. Catal.* 354, 3275–3282. doi: 10.1002/adsc.201200474

Nguyen, H. H. T., Shiemke, A. K., Jacobs, S. J., Hales, B. J., Lidstrom, M. E., and Chan, S. I. (1994). The nature of the copper ions in the membranes containing the particulate methane monooxygenase from *Methylococcus capsulatus* (Bath). *J. Biol. Chem.* 269, 14995–15005.

Olah, G. A., Fung, A. P., and Keumi, T. (1981). Oxyfunctionalization of hydrocarbons. 11. hydroxylation of benzene and alkylbenzenes with hydrogen peroxide in hydrogen fluoride/boron trifluoride. *J. Org. Chem.* 46, 4305–4306. doi: 10.1021/jo00334a046

Ottenbacher, R. V., Talsi, E. P., and Bryliakov, K. P. (2020). Recent progress in catalytic oxygenation of aromatic C–H groups with the environmentally benign oxidants H_2O_2 and O_2. *Appl. Organometal. Chem. e.* 34:e5900. doi: 10.1002/aoc.5900

Ottenwaelder, X., Rudd, D. J., Corbett, M. C., Hodgson, K. O., Hedman, B., and Stack, T. D. P. (2006). Reversible O–O bond cleavage in copper–dioxygen isomers: impact of anion basicity. *J. Am. Chem. Soc.* 128, 9268–9269. doi: 10.1021/ja061132g

Pignatello, J. J., Oliveros, E., and Mackay, A. (2006). Advanced oxidation processes for organic contaminant destruction based on the fenton reaction and related chemistry. *Crit. Rev. Environ. Sci. Technol.* 36, 1–84. doi: 10.1080/10643380500326564

Raba, A., Cokoja, M., Herrmann, W. A., and Kuhn, F. E. (2014). Catalytic hydroxylation of benzene and toluene by an iron complex bearing a chelating di-pyridyl-di-NHC ligand. *Chem. Commun.* 50, 11454–11457. doi: 10.1039/C4CC02178A

Rach, S. F., and Kühn, F. E. (2009). Nitrile ligated transition metal complexes with weakly coordinating counteranions and their catalytic applications. *Chem. Rev.* 109, 2061–2080. doi: 10.1021/cr800270h

Ramu, R., Wanna, W. H., Janmanchi, D., Tsai, Y. F., Liu, C. C., Mou, C. Y., et al. (2017). Mechanistic study for the selective oxidation of benzene and toluene catalyzed by $Fe(ClO_4)_2$ in an H_2O_2-H_2O-CH_3CN system. *Mol. Catal.* 441, 114–121. doi: 10.1016/j.mcat.2017.08.006

Rouquerol, J., Avnir, D., Fairbridge, C. W., Everett, D. H., Haynes, J. M., Pernicone, N., et al. (1994). Recommendations for the characterization of porous solids (Technical Report). *Pure Appl. Chem.* 66:1739. doi: 10.1351/pac199466081739

Sawyer, D. T., Sobkowiak, A., and Matsushita, T. (1996). Metal [ML_x; M = Fe, Cu, Co, Mn]/hydroperoxide-Induced activation of dioxygen for the oxygenation of hydrocarbons: oxygenated fenton chemistry. *Acc. Chem. Res.* 29, 409–416. doi: 10.1021/ar950031c

Shul'pin, G. B., Ishii, Y., Sakaguchi, S., and Iwahama, T. (1999). Oxidation with the "O_2-H_2O_2–vanadium complex—pyrazine-2-carboxylic acid" reagent. *Russ. Chem. Bull.* 48, 887–890. doi: 10.1007/BF02494631

Shul'pin, G. B., Kozlov, Y. N., Shul'pina, L. S., and Petrovskiy, P. V. (2010). Oxidation of alkanes and alcohols with hydrogen peroxide catalyzed by complex $Os_3(CO)_{10}(\mu\text{-}H)_2$. *Appl. Organometal. Chem.* 24, 464–472. doi: 10.1002/aoc.1641

Shul'pina, L. S., Takaki, K., Strelkova, T. V., and Shul'pin, G. B. (2008). Benzene oxidation with hydrogen peroxide catalyzed by soluble and heterogenized copper compounds. *Petro. Chem.* 48, 219–222. doi: 10.1134/S0965544108030080

Siegmund, H. U., and Kaufman, S. (1991). Hydroxylation of 4-methylphenylalanine by rat liver phenylalanine hydroxylase. *J. Biol. Chem.* 266, 2903–2910.

Suib, S. L., Prech, J., Cejka, J., Kuwahara, Y., Mori, K., and Yamashita, H. (2020). Some novel porous materials for selective catalytic oxidations. *Mater. Today* 32, 244–259. doi: 10.1016/j.mattod.2019.06.008

Thibon, A., Jollet, V., Ribal, C., Sénéchal-David, K., Billon, L., Sorokin, A. B., et al. (2012). Hydroxylation of aromatics with the help of a non-haem FeOOH: a mechanistic study under single-turnover and catalytic conditions. *Chem. Eur. J.* 18, 2715–2724. doi: 10.1002/chem.201102252

Thommes, M., Kaneko, K., Neimark, A. V., Olivier, J. P., Rodriguez-Reinoso, F., Rouquerol, J., et al. (2015). Physisorption of gases, with special reference to the evaluation of surface area and pore size distribution (IUPAC Technical Report). *Pure Appl. Chem.* 87:1051. doi: 10.1515/pac-2014-1117

Walling, C. (1975). Fenton's reagent revisited. *Acc. Chem. Res.* 8, 125–131. doi: 10.1021/ar50088a003

Wang, V. C. C., Maji, S., Chen, P. P. Y., Lee, H. K., Yu, S. S. F., and Chan, S. I. (2017). Alkane oxidation: methane monooxygenases, related enzymes, and their biomimetics. *Chem. Rev.* 117, 8574–8621. doi: 10.1021/acs.chemrev.6b00624

Wanna, W. H., Janmanchi, D., Thiyagarajan, N., Ramu, R., Tsai, Y. F., Pao, C. W., et al. (2019a). Selective catalytic oxidation of benzene to phenol by a vanadium oxide nanorod (V_{nr}) catalyst in CH_3CN using $H_2O_{2(aq)}$ and pyrazine-2-carboxylic acid (PCA). *New J. Chem.* 43, 17819–17830. doi: 10.1039/C9NJ02514F

Wanna, W. H., Ramu, R., Janmanchi, D., Tsai, Y. F., Thiyagarajan, N., and Yu, S. S. F. (2019b). An efficient and recyclable copper nano-catalyst for the selective oxidation of benzene to *p*-benzoquinone (*p*-BQ) using $H_2O_{2(aq)}$ in CH_3CN. *J. Catal.* 370, 332–346. doi: 10.1016/j.jcat.2019.01.005

Wu, C. K., Yin, M., O'brien, S., and Koberstein, J. T. (2006). Quantitative analysis of copper oxide nanoparticle composition and structure by X-ray photoelectron spectroscopy. *Chem. Mater.* 18, 6054–6058. doi: 10.1021/cm061596d

Yalymov, A. I., Bilyachenko, A. N., Levitsky, M. M., Korlyukov, A. A., Khrustalev, V. N., Shul'pina, L. S., et al. (2017). High catalytic activity of heterometallic (Fe_6Na_7 and Fe_6Na_6) cage silsesquioxanes in oxidations with peroxides. *Catalysts* 7:101. doi: 10.3390/catal7040101

Yamaguchi, S., Ohnishi, T., Miyake, Y., and Yahiro, H. (2015). Effect of water added into acetonitrile solvent on oxidation of benzene with hydrogen peroxide over iron complexes encapsulated in zeolite. *Chem. Lett.* 44, 1287–1288. doi: 10.1246/cl.150479

Yang, C. L., Lin, C. H., Luo, W. I., Lee, T. L., Ramu, R., Ng, K. Y., et al. (2017). Mechanistic study of the stereoselective hydroxylation of $[2-^2H_1,3-^2H_1]$ butanes catalyzed by cytochrome P450 BM3 variants. *Chem. Eur. J.* 23, 2571–2582. doi: 10.1002/chem.201603956

You, X., Wei, Z., Wang, H., Li, D., Liu, J., Xu, B., et al. (2014). Synthesis of two copper clusters and their catalysis towards the oxidation of benzene into phenol. *RSC Adv.* 4, 61790–61798. doi: 10.1039/C4RA12832J

Zhang, X., Zhang, T., Li, B., Zhang, G., Hai, L., Ma, X., et al. (2017). Direct synthesis of phenol by novel [FeFe]-hydrogenase model complexes as catalysts of benzene hydroxylation with H_2O_2. *RSC Adv.* 7, 2934–2942. doi: 10.1039/C6RA27831K

Zhao, X. T., Yan, Y. Y., Mao, L., Fu, M. C., Zhao, H. R., Sun, L. S., et al. (2018). A relationship between the V^{4+}/V^{5+} ratio and the surface dispersion, surface acidity, and redox performance of V_2O_5-WO_3/TiO_2 SCR catalysts. *RSC Adv.* 8, 31081–31093. doi: 10.1039/C8RA02857E

Zhou, T., Zhang, J., Ma, Y. Y., Gao, X., Xue, Q., Gao, Y., et al. (2020). A bicadmium-substituted polyoxometalate network based on a vanadosilicate cluster for the selective oxidation of styrene to benzaldehyde. *Inorg. Chem.* 59, 5803–5807. doi: 10.1021/acs.inorgchem.0c00072

Zoubi, M. A., Farag, H. K., and Endres, F. (2009). Sol–gel synthesis of vanadium pentoxide nanoparticles in air- and water-stable ionic liquids. *J. Mate. Sci.* 44, 1363–1373. doi: 10.1007/s10853-008-3004-4